JACS
JOURNAL OF THE AMERICAN CHEMICAL SOCIETY

Article

pubs.acs.org/JACS

Ultrahigh-Water-Content Supramolecular Hydrogels Exhibiting Multistimuli Responsiveness

Eric A. Appel,[†] Xian Jun Loh,[†] Samuel T. Jones,[†] Frank Biedermann,[†] Cecile A. Dreiss,[‡] and Oren A. Scherman*,[†]

[†]Melville Laboratory for Polymer Synthesis, Department of Chemistry, Cambridge University, Lensfield Road, Cambridge CB2 1EW, U.K.

[‡]Institute of Pharmaceutical Science, King's College London, Franklin-Wilkins Building, 150 Stamford Street, London SE1 9NH, U.K.

Supporting Information

ABSTRACT: Hydrogels are three-dimensional networked materials that are similar to soft biological tissues and have highly variable mechanical properties, making them increasingly important in a variety of biomedical and industrial applications. Herein we report the preparation of extremely high water content hydrogels (up to 99.7% water by weight) driven by strong host–guest complexation with cucurbit[8]uril (CB[8]). Cellulosic derivatives and commodity polymers such as poly(vinyl alcohol) were modified with strongly binding guests for CB[8] ternary complex formation (K_{eq} = 10^{12} M^{-2}). When these polymers were mixed in the presence of CB[8], whereby the overall solid content was 90% cellulosic, a lightly colored, transparent hydrogel was formed instantaneously. The supramolecular nature of these hydrogels affords them with highly tunable mechanical properties, and the dynamics of the CB[8] ternary complex cross-links allows for rapid self-healing of the materials after damage caused by deformation. Moreover, these hydrogels display responsivity to a multitude of external stimuli, including temperature, chemical potential, and competing guests. These materials are easily processed, and the simplicity of their preparation, their availability from inexpensive renewable resources, and the tunability of their properties are distinguishing features for many important water-based applications.

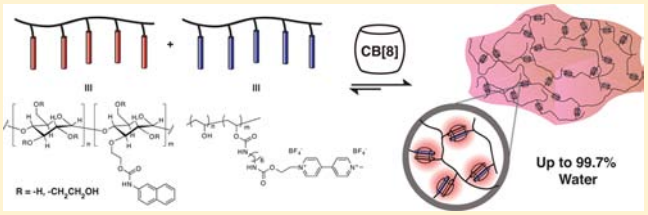

INTRODUCTION

Hydrogels are an important class of material that can be prepared using either a covalent or a noncovalent approach.[1−4] Most covalently cross-linked polymer hydrogels are brittle, have poor transparency, and lack the ability to self-heal once the network is broken.[5] These shortcomings have been addressed by employing dynamic and reversible noncovalent interactions as the structural cross-links in hydrogels (*direct* formation) or by driving nanofiber formation, whose entanglement subsequently leads to hydrogel formation (*indirect* formation).[6,7] There are myriad small molecules that self-assemble into long fibers, leading to hydrogel formation. An excellent example is the series of amphiphilic peptides developed by Stupp and coworkers.[8] Relatively strong hydrogels (G' = 1 kPa) with low loadings of material relative to water (0.5 wt % peptide + 0.5 wt % $CaCl_2$) can be prepared in this manner.[9] There are, however, far fewer examples of *direct* hydrogel formation, especially those with high water content (>98%).

From the precedent of supramolecular polymers,[10] it is clear that only very few specific and directional noncovalent systems that function in aqueous media exist. These include host–guest interactions of macrocyclic hosts, including cyclodextrins (CDs) and cucurbit[*n*]urils (CB[*n*]s), as well as hydrophobic, ionic, and some metal–ligand interactions. Several attempts have been made previously to develop hydrogels from CDs, but they have been intrinsically limited by the low binding affinity of CDs to their guests, which has resulted in poor mechanical properties.[11,12] Ionic interactions[13−15] are extremely sensitive to the ionic strength of the aqueous medium and often to changes in pH, while the use of transition metals in metal–ligand pairs must be avoided in many applications because of toxicity and environmental concerns. A variety of natural systems have been reported, including self-assembled chitosan-based hydrogels that can be formed at high pH[16] and alginate-based hydrogels cross-linked by multivalent cations (e.g., Ca^{2+} and Ba^{2+}) in a mild gelling reaction.[17] Thermally activated hydrogels formed by hydrophobic association of block copolymers, typically containing two or more blocks displaying a lower critical solution temperature, have been extensively studied.[18] Although these materials, especially poly(*N*-isopropylacrylamide) and Pluronics, have demonstrated potential for biomedical applications on account of their spontaneous formation at physiological temperature and biocompatibility, they are intrinsically limited to a narrow operating temperature range. Furthermore, to the best of our knowledge, all previous examples of supramolecular hydrogels formed by a *direct* formation mechanism have been reported to contain greater than 2 wt % solids.

Received: May 8, 2012
Published: June 14, 2012

   dx.doi.org/10.1021/ja3044568 | *J. Am. Chem. Soc.* 2012, 134, 11767−11773

Our approach involves the use of simple, inexpensive, and commercially available materials from renewable feedstocks coupled with a strong, reversible, and stimuli-responsive CB[8]-based 1:1:1 ternary binding motif. CB[n] (n = 5−8, 10) are a family of macrocyclic host molecules consisting of methylene-linked oligomers of glycoluril that have a symmetric "barrel" shape with two identical portal regions laced by ureidocarbonyl oxygens. The number of glycoluril units determines the size of the CB[n] cavity without affecting the height of the molecular container (∼0.9 nm), similar to the CD family, and these materials have recently been screened for toxicity and found to be generally nontoxic.[19,20] While smaller homologues of the CB[n] family (i.e., CB[5], CB[6], and CB[7]) are capable of binding single guests (typically cationic amines, metal, or imidazolium ions),[21−23] CB[8] has a larger cavity volume and can simultaneously accommodate two guests.[24,25] An electron-deficient first guest such as a methyl viologen (MV) derivative and an electron-rich second guest such as a naphthalene (Np) derivative form a stable 1:1:1 ternary complex with CB[8] through multiple noncovalent interactions acting synergistically. This results in exceptionally high equilibrium binding affinities ($K_a \leq 10^{14}$ M^{-2}).[26] The ternary complex forms in a stepwise binding process whereby the electron-poor guest enters first (K_{a1}) followed by the electron-rich guest (K_{a2}), whose entry is accompanied by the quantitative formation of a new visible absorbance on account of formation of a charge-transfer complex between the MV and Np groups.

The utility of CB[8] as a linking agent has been demonstrated in polymeric systems wherein two end-functionalized polymers could be reversibly complexed into a supramolecular block copolymer.[27−29] Moreover, systems have been reported previously that exploit CB[8]-based interactions between multivalent peptides[30] and with side-chain-functionalized polymers for the controlled folding of single polymer chains,[31] complexation of small molecules,[32] and preparation of composite materials with functionalized metal nanoparticles.[33,34] We previously reported the preparation of supramolecularly cross-linked viscoelastic materials from relatively low molecular weight synthetic polymers with CB[8] that formed viscous materials above 5 wt % loading.[35] Herein we build on our previous report by altering the polymer backbone to utilize commercially available commodity polymers and renewable cellulosic derivatives along with facile, rapid, and scalable conjugation techniques to prepare ultrahigh-water-content hydrogels (up to 99.7%; Figure 1). Furthermore, the well-known stimuli-responsive nature of the ternary complex and the ease of synthesis of the various components make this system well-suited for a variety of important biomedical and industrial applications.

RESULTS AND DISCUSSION

Synthesis and Characterization of Functionalized Polymeric Materials. A cellulose-based scaffold, hydroxyethyl cellulose (HEC), with a number-average molecular weight (M_n) of 1.3 MDa, was chosen as the primary polymeric material for preparation of hydrogels on account of its high solubility, molecular weight, and hydroxyl functionality. To maximize the use of the renewable cellulosic scaffold, the HEC was readily functionalized using commercially available 2-naphthyl isocyanate in a one-step reaction performed at ambient temperature in *N*-methylpyrrolidone (NMP) using dibutyltin dilaurate (TDL) as a catalyst (Figure 2a).[36] The excess isocyanate was readily removed by precipitation of the naphthyl-functionalized

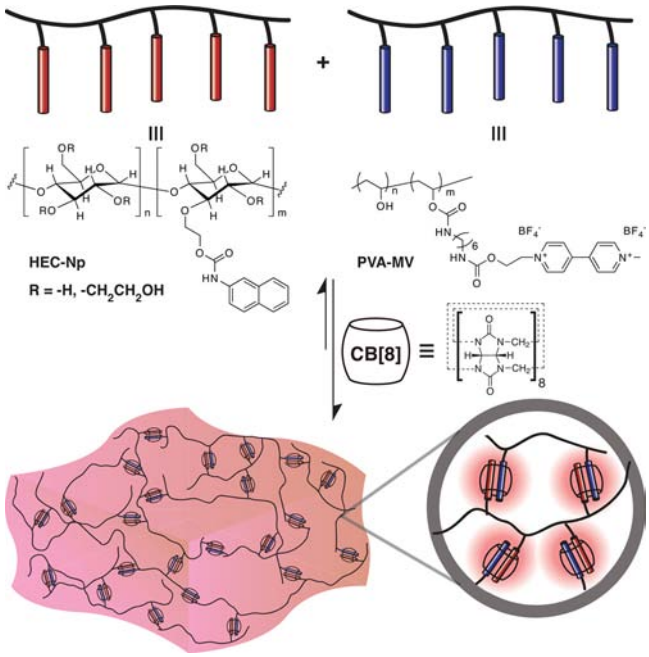

Figure 1. Schematic representation of a supramolecular hydrogel prepared through addition of cucurbit[8]uril to a mixture of multivalent first- and second-guest-functionalized polymers in water.

cellulose (HEC-Np). This simple method can be extended to a variety of other isocyanate-functionalized second guests that can be prepared either by employing diphenylphosphoryl azide (DPPA)[37] with carboxylic acids via thermal Curtius rearrangement or by reaction of triphosgene with amines.[36] Furthermore, an MV unit containing a hydroxyl group, 1-(2-hydroxyethyl)-1′-methyl-4,4′-bipyridine-1,1′-diium di(tetrafluoroborate), was reacted with an excess of 1,6-hexamethylene diisocyanate (HDI) to form the monofunctionalized addition product carrying one remaining isocyanate group for subsequent reaction (MV-NCO).[36] MV-NCO was conjugated to poly(vinyl alcohol) (PVA; M_n = 205 kDa), a commercially available commodity polymer, using conditions similar to those mentioned above, affording the MV-functionalized polymer PVA-MV (Figure 2b). These synthetic protocols are facile, rapid, and easily scaled.

Self-Assembly of Multivalent Polymers To Form Hydrogels. Isothermal titration calorimetry (ITC) is a powerful physical technique for measuring solution binding thermodynamics and stoichiometry that has been utilized previously to measure K_{eq} values in CB[8] host−guest systems.[26,30,38−40] With a range of multivalent polymers in hand, the quantitative investigation of their respective binding thermodynamic parameters was carried out utilizing ITC, and Table 1 displays the complete thermodynamic data for second-guest binding based on the concentration of functional units (i.e., not on the polymer concentration).

ITC measurements were carried out on PVA-MV both with a monovalent small molecule, 2-naphthol (NpOH), and with HEC-Np polymer in the presence of CB[8] in order to identify the effect on binding stemming from steric hindrance of the polymeric backbones. Likewise, measurements were carried out on HEC-Np polymer with a monovalent small molecule, dimethyl viologen (M_2V). In the case of polymer−polymer binding, the multivalent binding interactions were found to be noncooperative, i.e., the strength of each binding interaction is independent of all others. The resulting isotherm fit extremely

dx.doi.org/10.1021/ja3044568 | J. Am. Chem. Soc. 2012, 134, 11767−11773

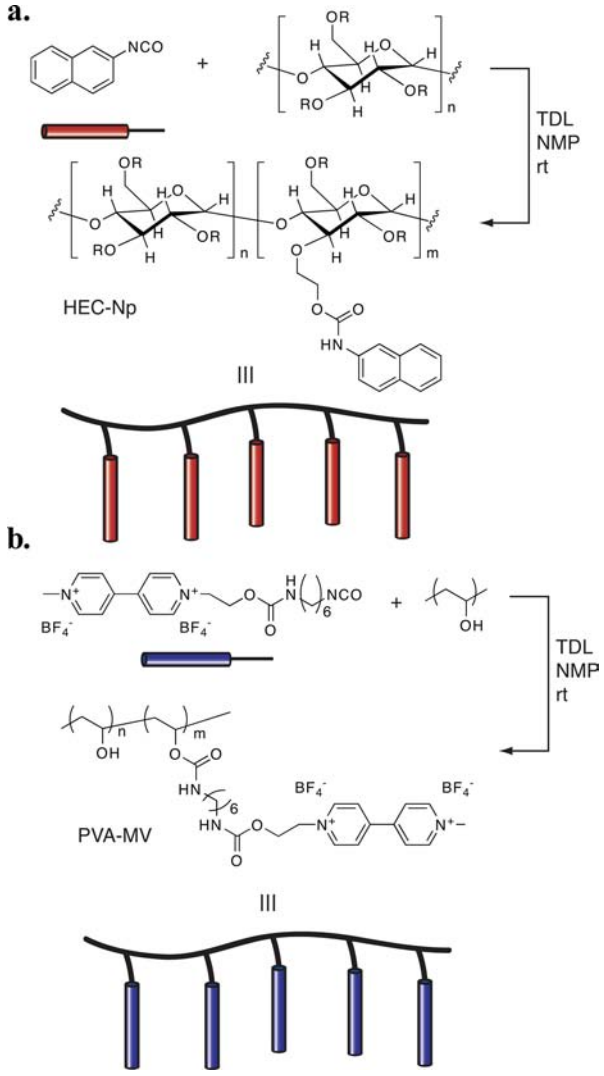

Figure 2. Synthetic schemes for the preparation of (a) HEC-Np and (b) PVA-MV using isocyanate coupling catalyzed by dibutyltin dilaurate (TDL) in *N*-methylpyrrolidone (NMP).

well to a one-set-of-sites binding model with an inflection point at an MV:Np:CB[8] molar ratio of 1:1:1 (see the Supporting Information). The presence of the inflection point at perfect 1:1:1 stoichiometry verified that all of the Np and MV units were accessible and took part in binding interactions. No significant difference between the binding constants for the polymeric entities and their corresponding small molecules was observed, indicating that there was no observable effect on the binding from steric hindrance arising from the polymer backbone.

Simple mixing of an aqueous solution of HEC-Np (0.5 wt %) with a solution of PVA-MV (0.05 wt %) containing an MV:CB[8] loading of 1:1 (PVA-MV@CB[8]) instantaneously produced a light-orange-colored, transparent hydrogel (Figure 3d). The orange color is inherent to the MV:Np:CB[8] ternary

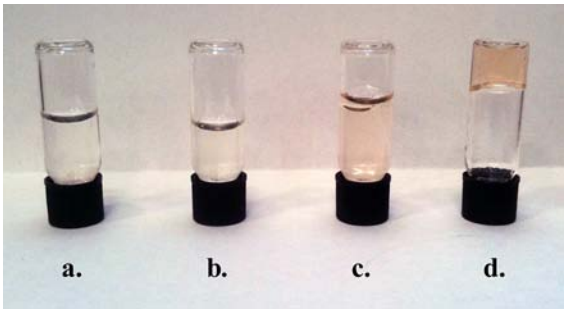

Figure 3. Inverted vial tests demonstrating the formation of the hydrogel from the mixture of HEC-Np (0.5 wt %), PVA-MV (0.05 wt %), and CB[8] (0.05 wt %) exclusively. (a) HEC-Np. (b) HEC-Np and PVA-MV. (c) HEC-Np, PVA-MV, and CB[7]. (d) HEC-Np, PVA-MV, and CB[8].

complex and is a product of the charge-transfer complex between the electron-poor MV and electron-rich Np moieties within the CB[8] cavity. At this point we observed that the hydrogels were "squishy", indicating a highly elastic nature, and also that they were able to self-heal instantaneously after the hydrogel was completely torn and the pieces were brought back into contact with one another (see below). Furthermore, the low amount of Np functionality present on the HEC-Np polymers (0.15 mmol of Np/g of HEC-Np) meant that the solid content of these hydrogels (0.06 wt %) was primarily cellulosic (~90 wt %). These materials, therefore, truly were formed primarily from renewable resources.

Additionally, there was a clear dependence of hydrogel formation on the presence of all three components of the ternary complex, as only the system with Np, MV, and CB[8] formed a hydrogel. A lack of any one of the components (Figure 3a,b) or replacing CB[8] with CB[7], whose cavity is large enough to encapsulate only MV alone (Figure 3c), did not produce hydrogels.

Rheological Characterization of the Supramolecular Hydrogels. Rheological measurements demonstrated no observable difference in the rheology of HEC (0.5 wt %) upon conjugation of the Np moiety (Figure 4a), indicating that conjugation of hydrophobic units to the HEC polymer does not lead to enhanced interchain association, corroborating aforementioned observations (see the Supporting Information). Strain-dependent oscillatory rheology of the materials formed through a titration of PVA-MV@CB[8] into an aqueous solution of HEC-Np (0.5 wt %) demonstrated that addition of only 0.05 wt % PVA-MV@CB[8] is required for hydrogel formation (Figure 4a). Varying the relative loading of HEC-Np to PVA-MV@CB[8] can produce materials with a large range

Table 1. Thermodynamic Data for Second-Guest Binding of Functionalized Polymers

entry	MV	Np	K_a (M^{-1})[a]	ΔG (kcal/mol)[b]	ΔH (kcal/mol)[a]	$-T\Delta S$ (kcal/mol)[c]
1	PVA-MV	HEC-Np	$(6.87 \pm 0.87) \times 10^5$	-33.3 ± 0.1	-7.6 ± 0.2	25.7 ± 0.2
2	PVA-MV	NpOH	$(1.10 \pm 0.03) \times 10^5$	-28.8 ± 0.1	-6.8 ± 0.2	21.9 ± 0.2
3	M_2V	HEC-Np	$(1.07 \pm 0.16) \times 10^5$	-28.7 ± 0.1	-24.5 ± 0.2	4.2 ± 0.2

[a]Mean values measured from at least three ITC experiments at 25 °C in 10 mM phosphate-buffered saline (pH 7.0). [b]Gibbs free energy values were calculated from the K_a values. [c]Entropic contributions to ΔG were calculated from the K_a and ΔH values.

dx.doi.org/10.1021/ja3044568 | J. Am. Chem. Soc. 2012, 134, 11767−11773

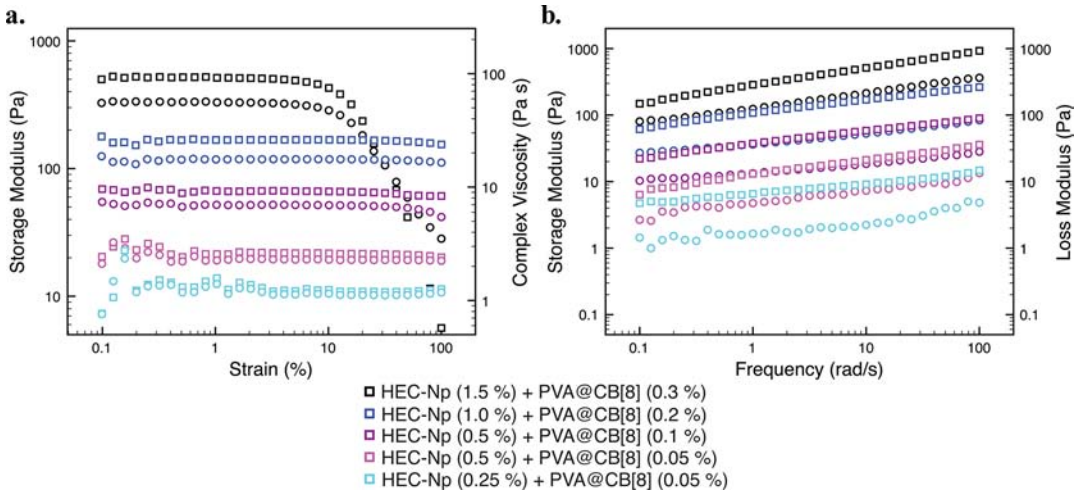

Figure 4. Oscillatory rheological analysis of the hydrogels demonstrating the effect of HEC-Np loading and the relative loading of HEC-Np to PVA-MV@CB[8] at 20 °C. (a) Storage modulus and complex viscosity obtained from a strain-amplitude sweep performed at 10 rad/s. (b) Storage and loss moduli obtained from a frequency sweep performed at 5% strain. Squares refer to the left axis and circles to the right axis. The legend shows the loadings of polymer constituents in wt %.

of mechanical properties (Figure 4). Moreover, all of the materials prepared displayed an extremely broad linear viscoelastic region, indicating that these materials have a broad processing region. Only at higher loadings of HEC-Np (1.5 wt %) was a deviation from linear viscoelasticity observed as a breakdown of the hydrogel structure at strain amplitudes above 10%, with large decreases in oscillatory shear modulus and complex viscosity. This is highly unique among supramolecular hydrogels, as these materials typically display breakdown of their structures at lower strains (below 10%).[15]

Frequency-dependent rheological characterizations performed in the linear viscoelastic region are shown in Figure 4b. The frequency dependence of the storage and loss oscillatory shear moduli (G' and G'', respectively) clearly identifies hydrogel-like behavior, as the G' and G'' curves are linear and parallel with G' is dominant across the whole range of frequencies studied (Figure 4b). In general, these hydrogels are soft (G' = 0.5 kPa at 1.5 wt % loading of HEC-Np) and display linear "shear-thinning" behavior, yet the range of materials produced are highly elastic ($\tan \delta = G'/G'' \approx 0.25$). Highly elastic materials ($\tan \delta \leq 0.25$) are obtained even at extremely high water content (99.7%). Moreover, the complex viscosity and mechanical properties of the material can be tuned over 2 orders of magnitude (Figure 4b).

According to steady-shear measurements, as demonstrated in Figure 5, the hydrogels are shear-thinning (η = 200 → 0.4 Pa s from $\dot{\gamma}$ = 0.1 → 100 s^{-1}), which is consistent with previous observations for dynamically associative cross-linked materials.[35] It should be noted here that the materials clearly do not follow the Cox–Merz rule, an empirical rule stating that the viscosity from steady-shear measurements in s^{-1} (Figure 5) should overlay the complex viscosity from the dynamic frequency sweep in rad/s (see the Supporting Information). The dynamic frequency sweep identified linear shear thinning behavior, while the steady-shear measurements demonstrated much more complicated rate-dependent behavior. The discrepancy is expected for dynamically cross-linked materials, as shear can induce reorganization of the network structure through deformation of the material while dynamic oscillatory measurements leave the network intact. Interestingly, however, materials containing between 0.25 and 0.5 wt % HEC-Np

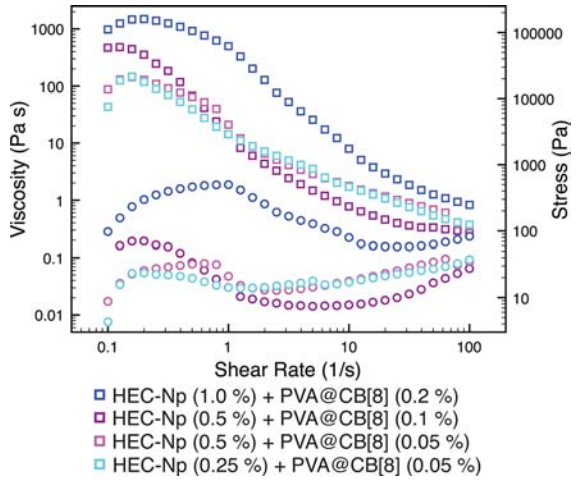

Figure 5. Steady-shear rheological measurements of the hydrogels demonstrating the response of the supramolecular hydrogels to constant-shear-induced deformation at 20 °C. The symbols and legend denotations are as above.

demonstrated very little difference in their shear-dependent viscosities. Only at very low shear rates (below 0.3 s^{-1}) did higher loading demonstrate a higher viscosity, as the materials exhibited an interesting response to shear. At HEC-Np (1.0 wt %), an increase in material properties was observed across the entire range of shear rates studied.

When the stress response of the materials to the imposed shear rate was plotted, an apparent "oscillation" was observed in the stress response covering the range of shear rates measured. This response is reminiscent of the shear stress versus shear rate behavior for materials exhibiting the spurt effect typically observed for wormlike micelles, as described by McLeish and Ball[41] and Doi and Edwards.[42]

The temperature-dependent rheological behavior was characterized up to 75 °C (Figure 6), where evaporation of water from the hydrogel samples in the parallel-plate geometry became problematic. Throughout this temperature range, the complex viscosity decreased only slightly (η^* = 2 → 0.3 Pa s) as the materials lost some mechanical integrity ($\tan \delta$ = 0.25 →

dx.doi.org/10.1021/ja3044568 | J. Am. Chem. Soc. 2012, 134, 11767–11773

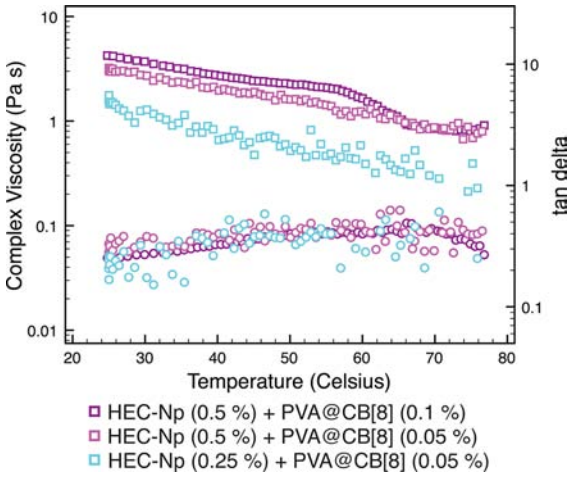

Figure 6. Thermal stability determined by a dynamic oscillatory temperature sweep test. The symbols and legend denotations are as above.

0.4). This decrease in the bulk mechanical properties with increasing temperature can be intuitively attributed to the concomitant decrease in the association constant of the dynamic ternary complex cross-links. These observations provided further evidence that the CB[8] ternary complex was responsible for the hydrogel structure and associated properties.

Step-rate measurements were performed to investigate the recovery of the hydrogel material properties following deformation at high shear rates. A high-magnitude shear rate ($\dot{\gamma}$ = 500 s^{-1}) was applied to break down the hydrogel structure, and then a low magnitude shear rate ($\dot{\gamma}$ = 0.05 s^{-1}) was used to monitor the rate and extent of recovery of the bulk material properties. Figure 7 clearly demonstrates the exceptionally fast

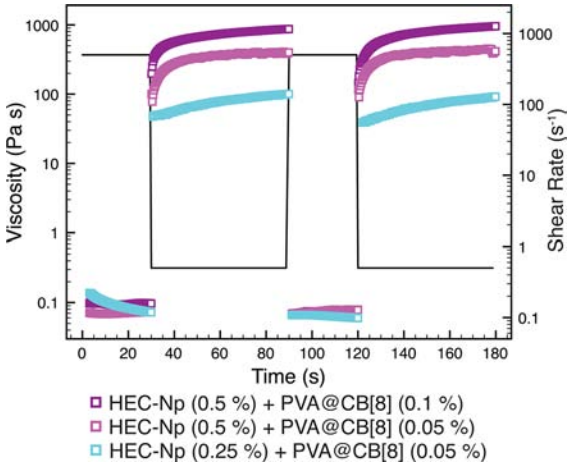

Figure 7. Step-rate time-sweep measurements displaying recovery of the hydrogel structure following high-magnitude deformation. The symbols and legend denotations are as above.

and complete recovery of viscosity after destruction of the gel structure in a matter of a few seconds. Previous measurements on the CB[8] ternary complex highlighted that the association kinetics are extremely rapid ($k_a \approx 10^8$ M^{-1} s^{-1}),[35] therefore leading us to hypothesize that this system would potentially lead to fast recovery of the mechanical properties in these hydrogels, which is consistent with our observations. The rate and extent of recovery were unchanged over several cycles of breaking and reforming, highlighting the reversible and robust nature of the noncovalently cross-linked hydrogel structure.

Structure of the Supramolecular Hydrogels. The structure of the hydrogels formed at a 0.5 wt % loading of HEC-Np were characterized by scanning electron microscopy (SEM) and small-angle neutron scattering (SANS). Figure 8 reveals that the microstructure of cryo-dried and lyophilized samples has a large dependence on the relative loading of HEC-Np and PVA-MV@CB[8]. A lower loading of PVA-MV@CB[8] (0.05 wt %) with the same 0.5 wt % loading of HEC-Np (Figure 8a) yielded much smaller pores after cryogenic freezing and lyophilization than the analogous hydrogel with a higher PVA-MV@CB[8] loading (0.1 wt %) (Figure 8b). This is presumably a result of the higher cross-link density and agrees with previously observed trends.[35]

SANS experiments were conducted using the D11 instrument at the Institut Laue-Langevin high-flux reactor source in Grenoble, France. Neutrons are sensitive to the nanometer range of length scales, and thus, a more refined picture of the molecular structure of the hydrogel could gained than that probed by SEM. The hydrogels were prepared in D_2O to allow for significant contrast between the aqueous phase and the hydrogel structure.

The scattering data for two hydrogels with differing loadings of PVA-MV@CB[8] relative to HEC-Np (0.5%) clearly superimpose (Figure 8c), showing no major changes in the nanostructure with the amount of PVA-MV@CB[8]. This observation indicates that the porous structures observed in the SEM images are actually formed in response to ice crystal formation during the cryogenic freezing process and that the structure of the fully solvated hydrogels can be attributed almost entirely to the loading of the cellulosic component. The scattering data can be appropriately described by a combination of the Debye–Bueche and Ornstein–Zerniche models, which are widely used to account for the scattering from gels and polymeric solutions.[43,44] The correlation length ξ could be fitted with values of 200 ± 30 Å, which are larger than those reported previously for similar polymeric gels. The large values are likely due to the exceptionally low loading of polymeric material relative to previously reported systems, yet they are consistent with the calculated mesh size based on distances between guest moieties along an extended, well-solvated polymer chain. The correlation length of the frozen-in structure, Ξ, could take a wide range of values between 500 and 1000 Å.

Multistimuli Responsivity of the Supramolecular Hydrogels. The CB[8] ternary complex, beyond providing a means for the preparation of self-assembled hydrogels, also imparts inherent stimuli responsiveness to the resulting materials in a tunable manner. These hydrogels are highly sensitive to specific external stimuli, including competing second guests and redox conditions. Addition of an excess of a competitive guest (e.g., 2,6-dihydroxynaphthalene or an aromatic solvent such as toluene) with mixing by vortex led to dissociation of the polymer network and complete loss of the bulk mechanical properties (Figure 9b,d). Upon addition of 2,6-dihydroxynaphthalene, the material began to flow yet retained it is light-orange color, as the competing guest also forms a colored charge-transfer complex similar to that formed with the pendant Np moieties on the HEC-Np polymer. On the contrary, toluene caused loss of both the mechanical properties and color, as toluene does not form a visible charge-

dx.doi.org/10.1021/ja3044568 | J. Am. Chem. Soc. 2012, 134, 11767–11773

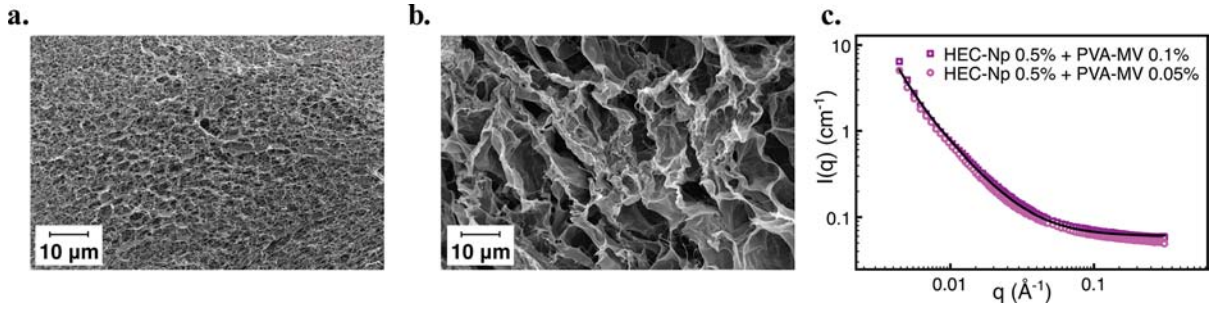

Figure 8. Characterization of the hydrogel microstructure. (a, b) SEM images of cryo-dried and lyophilized samples of (a) HEC-Np (0.5 wt %)/PVA-MV (0.05 wt %)/CB[8] (1 equiv) and (b) HEC-Np (0.5 wt %)/PVA-MV (0.1 wt %)/CB[8] (1 equiv). (c) SANS data for the same two hydrogels in D_2O.

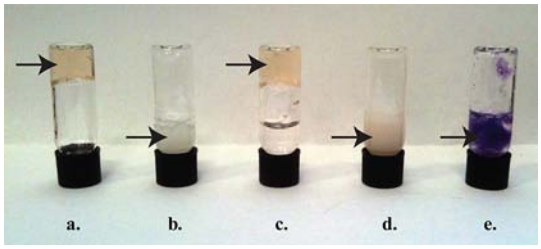

Figure 9. Hydrogels formed from (a) HEC-Np (0.5 wt %)/PVA-MV (0.1 wt %)/CB[8] (1 equiv) have variable responsiveness to perturbation in the presence of (b) toluene, (c) hexane, and (d) a competitive second guest (2,6-dihydroxynaphthalene) and also demonstrates responsiveness to (e) sodium dithionite reducing agent. In the case of (c) the intact hydrogel (indicated by the arrow) can be seen with its original color, while the hexane layer has flowed to the bottom of the vial.

transfer complex. In the case of toluene, partitioning of the toluene out of the aqueous layer after settling caused re-formation of the hydrogel. Moreover, when hexane was added with mixing by vortex, no alteration of the hydrogel properties was observed, as hexane, being a simple linear hydrocarbon, is not a suitable second guest for the CB[8] ternary complex (Figure 9c). Additionally, dilution with an equivalent volume of H_2O only slightly reduced the mechanical properties of the hydrogel (see Figure 4), highlighting that the observed decreases in mechanical properties are truly the result of specific interactions with the CB[8] ternary complex cross-links of the hydrogels.

A characteristic feature of this system is the one-electron reduction of MV, which reversibly breaks the ternary complex in favor of specific 2:1 $MV^{\bullet+}$:CB[8] complex formation.[34,45] We observed that this reversible one-electron redox couple can be utilized to alter the mechanical properties of the hydrogels using an externally applied stimulus. Addition of sodium dithionite, which is a good reducing agent for MV, yielded a blue low-viscosity solution ($MV^{\bullet+}$ is blue in color; Figure 9e). Although it would be intuitively possible for the PVA-MV polymer to cross-link with itself on account of 2:1 $MV^{\bullet+}$:CB[8] complex formation, only a low-viscosity solution was observed on account of the exceptionally low concentration of PVA-MV utilized in this system.

■ CONCLUSION

Self-assembled hydrogels with extremely high water content (up to 99.7%), highly tunable mechanical properties, and reversible responses to external stimuli have been prepared from simple materials synthesized in one step from widely available and inexpensive commercially available precursors from renewable resources. These materials are readily processed, and the simplicity of their preparation, their availability from inexpensive renewable resources, and the tunability of their mechanical properties are distinguishing features for many important water-based applications. A wide variety of other second guests exist for ternary complexation in this system and can be appended to myriad polymer backbones in the same way.[36] The diversity of both synthetic and natural materials and the additional flexibility with the polymer:-polymer:CB[8] loading ratio provide useful tools with which to tune the properties. This versatility is not only an asset for industrial development but also offers the opportunity to improve our understanding of challenging property−structure relationships and supramolecular structure formation.

■ EXPERIMENTAL SECTION

For hydrogel preparation, HEC-Np (5 mg) was first dissolved in water (0.5 mL) with stirring and mild heating. PVA-MV (0.1 mg) and CB[8] (0.1 mg) were then dissolved in water (0.5 mL) with ultrasonication (less than 5 min). The solutions were then mixed and shaken for ∼1 s as the hydrogel formed. ITC titration experiments were carried out on a Microcal VP-ITC instrument at 25 °C in 10 mM sodium phosphate buffer (pH 7). In a typical experiment, the host was in the sample cell at a concentration of 0.1 mM, and the guest was in the syringe at a 10-fold higher concentration. In the case of functionalized polymers, the concentration used was determined from the concentration of functional monomer units in solution and not the concentration of polymer. A titration consisted of 29 consecutive injections of 2−10 μL with at least 300 s intervals between injections. The first data point was removed from the data set prior to curve fitting. Heats of dilution were checked by titration well beyond saturation or by titration of the guest into a buffer solution and subtracted from the normalized enthalpies; they were relatively small in all cases. The data were analyzed with Origin 7.0 software using the one-set-of-sites model. Rheological characterization was performed using a TA Instruments ARES-LC controlled-strain rheometer fitted with a water bath set to 25 °C. Temperature sweeps were performed on a ramp from 25 to 75 °C at a rate of 10 °C/min. All measurements were performed using a 25 mm parallel-plate geometry and analyzed using TA Instruments TA Orchestrator software. SANS measurements were performed on the D11 installation at the high-flux reactor at the Institut Laue-Langevin in Grenoble, France. SEM images were obtained using a Leo 1530 variable-pressure scanning electron microscope using an InLens detector. SEM samples were prepared by direct freezing of the supramolecular hydrogels in liquid nitrogen followed by lyophilization. The resulting cryo-dried materials were imaged after sputtering. Full characterization and synthetic protocols are available in the Supporting Information.

■ ASSOCIATED CONTENT

Supporting Information

^{1}H NMR, GPC, ITC, and rheological measurements. This material is available free of charge via the Internet at http://pubs.acs.org.

■ AUTHOR INFORMATION

Corresponding Author

oas23@cam.ac.uk

Notes

The authors declare no competing financial interest.

■ ACKNOWLEDGMENTS

The authors acknowledge the Institut Laue-Langevin for use of their SANS facilities and especially Isabelle Grillo for help with the experiments and data reduction. This work was supported in part by Schlumberger, the Walters-Kundert Foundation, and an ERC Starting Investigator Grant (ASP*i*Re). X.J.L. thanks A*STAR for the postdoctoral fellowship.

■ REFERENCES

(1) Lutolf, M. P. *Nat. Mater.* **2009**, *8*, 451−453.
(2) Stuart, M. A. C.; Huck, W. T. S.; Genzer, J.; Mueller, M.; Ober, C.; Stamm, M.; Sukhorukov, G. B.; Szleifer, I.; Tsukruk, V. V.; Urban, M.; Winnik, F.; Zauscher, S.; Luzinov, I.; Minko, S. *Nat. Mater.* **2010**, *9*, 101−113.
(3) Lee, K. Y.; Mooney, D. J. *Chem. Rev.* **2001**, *101*, 1869−1879.
(4) Langer, R.; Tirrell, D. A. *Nature* **2004**, *428*, 487−492.
(5) Peppas, N. A.; Huang, Y.; Torres-Lugo, M.; Ward, J. H.; Zhang, J. *Annu. Rev. Biomed. Eng.* **2000**, *2*, 9−29.
(6) Wojtecki, R. J.; Meador, M. A.; Rowan, S. J. *Nat. Mater.* **2010**, *10*, 14−27.
(7) Estroff, L. A.; Hamilton, A. D. *Chem. Rev.* **2004**, *104*, 1201−1217.
(8) Hartgerink, J. D.; Beniash, E.; Stupp, S. I. *Science* **2001**, *294*, 1684−1688.
(9) Greenfield, M. A.; Hoffman, J. R.; de la Cruz, M. O.; Stupp, S. I. *Langmuir* **2010**, *26*, 3641−3647.
(10) Greef, T. F. A. D.; Smulders, M. M. J.; Wolffs, M.; Schenning, A. P. H. J.; Sijbesma, R. P.; Meijer, E. W. *Chem. Rev.* **2009**, *109*, 5687−5754.
(11) Wu, D. Q.; Wang, T.; Lu, B.; Xu, X. D.; Cheng, S. X.; Jiang, X. J.; Zhang, X. Z.; Zhuo, R. X. *Langmuir* **2008**, *24*, 10306−10312.
(12) Koopmans, C.; Ritter, H. *Macromolecules* **2008**, *41*, 7418−7422.
(13) Hunt, J. N.; Feldman, K. E.; Lynd, N. A.; Deek, J.; Campos, L. M.; Spruell, J. M.; Hernandez, B. M.; Kramer, E. J.; Hawker, C. J. *Adv. Mater.* **2011**, *23*, 2327−2331.
(14) Wang, Q.; Mynar, J. L.; Yoshida, M.; Lee, E.; Lee, M.; Okuro, K.; Kinbara, K.; Aida, T. *Nature* **2010**, *463*, 339−343.
(15) Mynar, J. L.; Aida, T. *Nature* **2008**, *451*, 895−896.
(16) Ta, H. T.; Dass, C. R.; Dunstan, D. E. *J. Controlled Release* **2008**, *126*, 205−216.
(17) Augst, A. D.; Kong, H. J.; Mooney, D. J. *Macromol. Biosci.* **2006**, *6*, 623−633.
(18) Loh, X. J.; Goh, S. H.; Li, J. *Biomacromolecules* **2007**, *8*, 585−593.
(19) Uzunova, V. D.; Cullinane, C.; Brix, K.; Nau, W. M.; Day, A. I. *Org. Biomol. Chem.* **2010**, *8*, 2037−2042.
(20) Hettiarachchi, G.; Nguyen, D.; Wu, J.; Lucas, D.; Ma, D.; Isaacs, L.; Briken, V. *PLoS One* **2010**, *5*, No. e10514.
(21) Zhao, N.; Liu, L.; Biedermann, F.; Scherman, O. A. *Chem.—Asian J.* **2010**, *5*, 530−537.
(22) Marquez, C.; Hudgins, R. R.; Nau, W. M. *J. Am. Chem. Soc.* **2004**, *126*, 5806−5816.
(23) Lagona, J.; Mukhopadhyay, P.; Chakrabarti, S.; Isaacs, L. *Angew. Chem., Int. Ed.* **2005**, *44*, 4844−4870.
(24) Day, A.; Arnold, A. P.; Blanch, R. J.; Snushall, B. *J. Org. Chem.* **2001**, *66*, 8094−8100.
(25) Kim, J.; Jung, I. S.; Kim, S. Y.; Lee, E.; Kang, J. K.; Sakamoto, S.; Yamaguchi, K.; Kim, K. *J. Am. Chem. Soc.* **2000**, *122*, 540−541.
(26) Rauwald, U.; Biedermann, F.; Deroo, S.; Robinson, C. V.; Scherman, O. A. *J. Phys. Chem. B* **2010**, *114*, 8606−8615.
(27) Rauwald, U.; Scherman, O. A. *Angew. Chem., Int. Ed.* **2008**, *47*, 3950−3953.
(28) Deroo, S.; Rauwald, U.; Robinson, C. V.; Scherman, O. A. *Chem. Commun.* **2009**, 644−646.
(29) Loh, X. J.; del Barrio, J.; Toh, P.; Lee, T.-C.; Jiao, D.; Rauwald, U.; Appel, E. A.; Scherman, O. A. *Biomacromolecules* **2012**, *13*, 84−91.
(30) Reczek, J. J.; Kennedy, A. A.; Halbert, B. T.; Urbach, A. R. *J. Am. Chem. Soc.* **2009**, *131*, 2408−2415.
(31) Appel, E. A.; Dyson, J.; del Barrio, J.; Walsh, Z.; Scherman, O. A. *Angew. Chem., Int. Ed.* **2012**, *51*, 4185−4189.
(32) Geng, J.; Jiao, D.; Rauwald, U.; Scherman, O. A. *Aust. J. Chem.* **2010**, *63*, 627−630.
(33) Zhang, J.; Coulston, R. J.; Jones, S. T.; Geng, J.; Scherman, O. A.; Abell, C. *Science* **2012**, *335*, 690−694.
(34) Coulston, R. J.; Jones, S. T.; Lee, T. C.; Appel, E. A.; Scherman, O. A. *Chem. Commun.* **2011**, *47*, 164−166.
(35) Appel, E. A.; Biedermann, F.; Rauwald, U.; Jones, S. T.; Zayed, J. M.; Scherman, O. A. *J. Am. Chem. Soc.* **2010**, *132*, 14251−14260.
(36) Biedermann, F.; Appel, E. A.; del Barrio, J.; Gruendling, T.; Barner-Kowollik, C.; Scherman, O. A. *Macromolecules* **2011**, *44*, 4828−4835.
(37) Shioiri, T.; Kunihiro, N.; Shunichi, Y. *J. Am. Chem. Soc.* **1972**, *94*, 6203−6205.
(38) Rajgariah, P.; Urbach, A. R. *J. Inclusion Phenom. Macrocyclic Chem.* **2008**, *62*, 251−254.
(39) Bush, M.; Bouley, N.; Urbach, A. *J. Am. Chem. Soc.* **2005**, *127*, 14511−14517.
(40) Heitmann, L. M.; Taylor, A. B.; Hart, P. J.; Urbach, A. R. *J. Am. Chem. Soc.* **2006**, *128*, 12574−12581.
(41) McLeish, T. C. B.; Ball, R. C. *J. Polym. Sci., Part B: Polym. Phys.* **1986**, *24*, 1735−1745.
(42) Doi, M.; Edwards, S. F. *The Theory of Polymer Dynamics*; Oxford University Press: Oxford, U.K., 1987.
(43) Benguigui, L.; Boue, F. *Eur. Phys. J. B* **1999**, *11*, 439−444.
(44) Horkay, F.; Basser, P. J.; Hecht, A. M.; Geissler, E. *Polymer* **2005**, *46*, 4242−4247.
(45) Lee, J. W.; Kim, K.; Choi, S.; Ko, Y. H.; Sakamoto, S.; Yamaguchi, K.; Kim, K. *Chem. Commun.* **2002**, 2692−2693.